Johann Radon Institute for
Computational and Applied Mathematics
Austrian Academy of Sciences (ÖAW)

Adaptive multi-parameter regularization in electrochemical impedance spectroscopy

M. Žic, S. Pereverzyev Jr.

RICAM-Report 2018-16

Adaptive multi-parameter regularization in electrochemical impedance spectroscopy

Mark Žic[a,*+] and Sergiy Pereverzyev Jr.[b*]

[a] A JESH-guest researcher at Johann Radon Institute for Computational and Applied Mathematics (RICAM), Altenbergerstrasse 69, A-4040 Linz, Austria
[b] Universitätsklinik für Neuroradiologie, Medizinische Universität Innsbruck, Anichstrasse 35, A-6020 Innsbruck, Austria

Abstract

Determination of the distribution function of relaxation times (DFRT) is an approach to the interpretation of Electrochemical Impedance Spectroscopy (EIS) measurements that maps these data into a function containing the timescale characteristics of the system under consideration. The extraction of such characteristics from noisy EIS measurements can be described by Fredholm interval equation of the first kind, which is known to be ill-posed and can be treated only with regularization techniques. Moreover, since only a finite number of EIS measurements may actually be performed, the above-mentioned equation appears as after application of a collocation method that needs to be combined with the regularization. Although in the regularization theory, such a combination has been studied and in principle can alone be used for solving the problems, it is suggested in the EIS literature to employ additional discretization of the corresponding Fredholm integral operator by quadrature or pseudo-spectral (projection) methods that of course, might increase the approximation error.

In the present study, we discuss how a regularized collocation of DFRT problem can be implemented such that all appearing quantities allow symbolic computations as sums of table integrals, and no additional discretization steps are required.

In the proposed implementation of the regularized collocation it is treated as a multi-parameter regularization, and another contribution of the present work is the adjustment of the previously proposed multiple parameter choice strategy to the context of DFRT problem. The resulting strategy is based on the aggregation of all computed regularized approximants, and can be in principle used in synergy with other methods for solving DFRT problem. We also report the results from the synthetic experiments showing that the proposed technique successfully reproduced known exact DFRT.

Keywords: EIS; DFRT; ill-posed problem; regularization; Python.

* Corresponding authors.
E-mail addresses: mzic@irb.hr (M. Žic) and sergiy.pereverzyev@i-med.ac.at (S. Pereverzyev Jr.).
+ Present address: Ruđer Bošković Institute, P.O. Box 180, 10000 Zagreb, Croatia.

1. Introduction

In electrochemical impedance spectroscopy (EIS), the experiments are usually interpreted fitting complex-valued impedance measurements $Z(\omega_j) = Z'(\omega_j) + iZ''(\omega_j), \quad j = 0,1,\dots,N-1,$ against chosen equivalent electrical circuit models. One of such models is known as the Voight circuit [1] and composed of a series of parallel capacitors C_m and resistors $R_m, m = 0,1,\dots,M-1,$ for which the impedance writes:

$$Z(\omega_j) = \sum_{m=0}^{M-1} \frac{R_m}{1 + i\omega_j \tau_m}, \qquad j = 0,1,\dots,N-1, \tag{1}$$

where $\tau_m = R_m C_m$. Note that sometimes an ohmic frequency independent part of the impedance is added to (1), which can potentially be directly estimated from impedance measurements for large angular frequencies ω and omitted here for simplicity.

Moreover, EIS experiments often cannot be described by a finite number of simple resistor-capacitor (RC) elements, because they involve distributed time constants. Then a Voigt circuit with an infinite number of RC elements can also be used to fit the impedance data ($Z(\omega)$), but instead of discrete values $R_m = \tau_m C_m^{-1}$ one should think the resistance variation $R = g(\tau)$ with time τ and deal with a continuous version of (1) such as

$$Z(\omega) = \int_0^\infty \frac{g(\tau)d\tau}{1 + i\omega\tau}, \tag{2}$$

where $g(\tau)$ describes the time relaxation characteristic of the electrochemical system under study.
Up to a certain extent $g(\tau)$ provides a circuit model-free representation of essential relaxation times that are directly connected to the charge transfer process, because not only Voigt circuit, but also other known circuit models, such as a constant phase element, Cole-Cole model, Davidson-Cole model, Warburg element, etc., can be discussed in terms of the equation (2).

Since we are interested in a real-valued solution $g(\tau)$ of (2), this equation can be reformulated into the system of equations with integral equations A_1, A_2:

$$\begin{cases} (A_1 g)(\omega) = \int_0^\infty \frac{g(\tau)d\tau}{1 + \omega^2\tau^2} = Z'(\omega), \\ (A_2 g)(\omega) = \int_0^\infty \frac{\omega\tau g(\tau)d\tau}{1 + \omega^2\tau^2} = -Z''(\omega), \end{cases} \tag{3}$$

where $Z'(\omega), Z''(\omega)$ are real and imaginary parts of $Z(\omega)$.

Observe that if instead of the whole function $Z(\omega)$ only the impedance measurements $Z(\omega_j) = Z'(\omega_j) + iZ''(\omega_j)$, $j = 0,1,\dots,N-1$, are available, then it reduces the system (3) to a collocation and can be abstractly written as

$$T_N A_1 g = T_N Z', \quad T_N A_2 g = -T_N Z'', \tag{4}$$

where T_N is the so-called sampling operator assigning to each function $F(\omega)$ a vector of its values at the collocation points ω_j, i.e., $T_N F = (F(\omega_0), F(\omega_1), \dots, F(\omega_{N-1}))$.

Recall that the collocation is a special form of discretization that arises when we replace the original problem, such as (3), by one in a finite dimensional space. In case of collocation this space is just the Euclidean space R^N of vectors $u = (u_0, u_1, \dots, u_{N-1})$, $v = (v_0, v_1, \dots, v_{N-1})$ equipped with a scalar product

$$< u, v >_{R^N} = \sum_{j=0}^{N-1} \gamma_j u_j v_j$$

and the corresponding norm $\|\cdot\|_{R^N}$; here the weights $\gamma_j, j = 0,1,\dots,\mathrm{N}-1$, are some positive numbers.

Note that if operators A_1, A_2 are considered to be acting from the space $L_2(0,\infty)$ of real-values square summable functions on $(0,\infty)$ then the equations (4), due to their finite dimension, are always solvable at least in the sense of least squares. Moreover, least square solutions of (4) can be reduced to the corresponding systems of *N* linear algebraic equations, such that no additional discretization is required and, as a result, no additional discretization error is introduced. Therefore, the impedance measurements considered as collocation data already hint at a way to approximate the solution of (2).

At the same time, in the literature one mainly finds two other approaches for approximate solving of (2). According to one of them, the integral operators A_1, A_2 in (4) are additionally discretized by means of quadrature formulas. This approach has been studied in [2-4].

The second approach, advocated in [5, 6], discretizes the operators A_1, A_2 in (4) by means of projection (pseudo-spectral) methods onto the subspaces of piecewise linear or radial basis functions.

In both above mentioned approaches the level of additional discretization, measuring by the number of knots of a quadrature formula or by the number of basics function, should be properly tuned. Such tuning is especially crucial in the case of noisy impedance measurements, when regularization techniques need to be employed to avoid numerical instabilities in solving (4). Then, according to the Regularization theory (see, e.g. [7]) the level of additional discretization of A_1, A_2 in (4) should be coordinated with the amount of regularization.

This topic has not been touched in the above mentioned literature. At the same time, this issue does not even appear if in (4) no additional discretization of the operators A_1, A_2 is introduced. Therefore, in the present paper we study an approach avoiding any additional discretization of the operators in (4). It is known (see, e.g. [2]) that the imaginary and real components $Z''(\omega_j)$, $Z'(\omega_j)$ of the impedance have different importance. Then it seems to be reasonable to treat the equations (4) with different amount of regularization. At the same time, in the above mentioned literature, the equations (4) are involved into a regularization scheme governed by only one regularization parameter that does not allow a desired flexibility in exercising the regularization. Therefore, in the present study, we follow [8] and employ a multi-parameter regularization. Moreover, we use the idea [8] of an aggregation of regularized solutions corresponding to different values of multiple regularization parameters that allows an automatic regularization in the form of a toolbox.

2. Theory

2.1 A multi-parameter regularization of the collocated impedance equations

In this section we analyze a methodology for joint regularization of the collocation equations (4) that leads to a multi-parameter regularization. The joint regularization can be formulated as the minimization of the objective functional

$$\Phi(g) := \lambda_1 \|T_N A_1 g - T_N Z'\|^2_{R_N} + \lambda_2 \|T_N A_2 g + T_N Z''\|^2_{R_N} + \|g\|^2_{L_2(0,\infty)}. \quad (5)$$

Here the first two terms are the measures of data misfit weighed with the regularization parameters $\lambda_1, \lambda_2 \subseteq (0, \infty)$. These misfits measures are combined in (5) with a regularization measure. In the spirit of the Tikhonov-Philips regularization the latter one is chosen as the norm of the solution space $L_2(0, \infty)$ generated by the scalar product

$$\langle \mathrm{f}, \mathrm{g} \rangle_{\mathrm{L}_2(0,\infty)} := \int_0^\infty f(\tau) g(\tau) d\tau, \quad f, g \subseteq L_2(0, \infty). \quad (6)$$

It is known, for example, from [8] that the regularized approximated solution $g_{\lambda_1,\lambda_2}(\tau)$ of (4) minimizing (5) can be found from the operator equation

$$\mathrm{g} + \lambda_1 (\mathrm{T_N A_1})^* \mathrm{T_N A_1 g} + \lambda_2 (\mathrm{T_N A_2})^* \mathrm{T_N A_2 g} = \lambda_1 (\mathrm{T_N} A_1)^* T_N Z' - \lambda_2 (T_N A_2)^* T_N Z'', \quad (7)$$

where $(T_N A_1)^*$ and $(T_N A_2)^*$ are the adjoins of $T_N A_1$ and $T_N A_2$ respectably. They are defined by the relations

$$\langle u, T_N A_1 f \rangle_{R^N} = \langle (T_N A_1)^* u, f \rangle_{L_2(0,\infty)}, \ \langle u, T_N A_2 f \rangle_{R^N} = \langle (T_N A_2)^* u, f \rangle_{L_2(0,\infty)}, \quad (8)$$

that should be satisfied for any $f \subseteq L_2(0,\infty)$ and $u = (u_0, u_1, \dots, u_{N-1}) \subseteq R^N$. In view of definition of $\langle\cdot,\cdot\rangle_{R^N}, T_N$ and (3) we have

$$\langle u, T_N A_1 f\rangle_{R^N} = \sum_{j=0}^{N-1} \gamma_j u_j \left(\int_0^\infty \frac{f(\tau)d\tau}{1+\omega_j^2\tau^2} \right) = \int_0^\infty \left(\sum_{j=0}^{N-1} \frac{\gamma_j u_j}{1+\omega_j^2\tau^2} \right) f(\tau)d\tau = \langle \sum_{j=0}^{N-1} \frac{1}{1+\omega_j^2\tau^2}\gamma_j u_j, f\rangle_{L_2(0,\infty)}.$$

Now from (8) we can conclude that for any $u = (u_0, u_1, \dots, u_{N-1}) \subseteq R^N$

$$(T_N A_1)^* u = \sum_{j=0}^{N-1} \frac{1}{1+\omega_j^2\tau^2}\gamma_j u_j. \tag{9}$$

On the other hand, by definition of the adjoint operator $(T_N A_1)^*$ it should be *N*-dimensional operator from $L_2(0,\infty)$ to R^N and, as such, it should allow the representation

$$(T_N A_1)^*(\cdot) = \sum_{j=0}^{N-1} l_i(\tau)\langle e^j, \cdot\rangle_{R^N}, \tag{10}$$

where $l_j \subseteq L_2(0,\infty), e^j \subseteq R^N$. Comparing this with (9) we arrive at the formulas

$$l_j(\tau) = \frac{1}{1+\omega_j^2\tau^2}, \qquad e^j = \left(e_0^j, e_1^j, \dots, e_{N-1}^j\right) \subseteq R^N, \qquad e_k^j = \delta_{kj}. \tag{11}$$

where δ_{kj} is the Kronecker delta, i.e. $\delta_{kj} = 0$ for $k \neq j$, and $\delta_{jj} = 1$.

By similar assignment, we can also obtain that

$$(T_N A_2)^*(\cdot) = \sum_{j=N}^{2N-1} l_j(\tau)\langle e^{j-N}, \cdot\rangle_{R^N}. \tag{12}$$

where

$$l_j(\tau) = \frac{\omega_{j-N}\tau}{1+\omega_{j-N}^2\tau^2}, \qquad j = N, N+1, \dots, 2N-1. \tag{13}$$

Now form (10)-(13) one can easily see that the solution of (7) admits the representation

$$g_{\lambda_1,\lambda_2}(\tau) = \sum_{j=0}^{N-1} g_j \frac{1}{1+\omega_j^2\tau^2} + \sum_{j=N}^{2N-1} g_j \frac{\omega_{j-N}\tau}{1+\omega_{j-N}^2\tau^2}. \tag{14}$$

The unknown coefficients $g_i = 0,1, \dots, 2N-1$, can be found from the following system of linear algebraic equations

$$\begin{cases} g_k + \lambda_1 \sum_{j=0}^{2N-1} a_{1,k,j} g_j = \lambda_1 \gamma_k Z'(\omega_k), & k = 0,1 \dots, N-1 \\ g_k + \lambda_2 \sum_{j=0}^{2N-1} a_{2,k,j} g_j = -\lambda_2 \gamma_{k-N} Z''(\omega_{k-N}), & k = N, N+1, \dots, 2N-1 \end{cases} \tag{15}$$

Where $a_{1,k,N+k} = \frac{\gamma_k}{2\omega_k}, \quad k = 0,1,\dots,N-1,$

$$a_{1,k,j} = \begin{cases} \int_0^\infty \frac{\gamma_k d\tau}{(1+\omega_k^2\tau^2)(1+\omega_j^2\tau^2)} = \frac{\pi\gamma_k}{2(\omega_k+\omega_j)}, \\ j = 0,1,2,\dots,N-1, \\ \int_0^\infty \frac{\gamma_k\ \omega_{j-N}\tau d\tau}{(1+\omega_k^2\tau^2)(1+\omega_{j-N}^2\tau^2)} = \frac{\gamma_k\omega_{j-N}}{(\omega_k^2-\omega^2{}_{j-N})}\ln\left(\frac{\omega_k}{\omega_{j-N}}\right), \\ j = N,\dots,2N-1; j \neq N+k, \end{cases}$$

and $a_{2,k,k-N} = \frac{\gamma_{k-N}}{2\omega_{k-N}}, \quad k = N, N+1, \dots, 2N-1,$

$$a_{2,k,j} = \begin{cases} \int_0^\infty \frac{\gamma_{k-N}\ \omega_{k-N}\tau d\tau}{(1+\omega_{k-N}^2\tau^2)(1+\omega_j^2\tau^2)} = \frac{\gamma_{k-N}\omega_{k-N}}{(\omega_{k-N}^2-\omega_j^2)}\ln\left(\frac{\omega_{k-N}}{\omega_j}\right), \\ j = 0,1,2,\dots,N-1; j \neq k-N, \\ \int_0^\infty \frac{\omega_{k-N}\omega_{j-N}\gamma_{k-N}\,\tau^2 d\tau}{(1+\omega_{k-N}^2\tau^2)(1+\omega_{j-N}^2\tau^2)} = \frac{\pi}{2}\gamma_{k-N}\frac{1}{\omega_{k-N}\omega_{j-N}(\omega_{k-N}+\omega_{j-N})}, \\ j = N, N+1, \dots, 2N-1. \end{cases}$$

From (14), (15) it is clear that for given λ_1, λ_2 the regularized approximate solution g_{λ_1,λ_2} of (4) can be constructed without additional discretization of the integral operators A_1, A_2. In the next section we discuss aggregation of g_{λ_1,λ_2} constructed for different values of the regularization parameters λ_1, λ_2.

2.2 Aggregation of g_{λ_1,λ_2} in weighted norms

It is known that the solution $g(\tau)$ of the impedance equation (2) may have singularities at $\tau = 0$. For example, in a constant-phase element model [9] the solution $g(\tau)$ has the form

$$g(\tau) = \frac{1}{2\pi\tau}\frac{\sin[(1-\varphi)\pi]}{\cosh\left[\varphi\ln\left(\frac{\tau}{\tau_0}\right)\right]-\cos[(1-\varphi)\pi]}, \varphi \subseteq (0,1),$$

and it is clear that $g(\tau) \to \infty$ with $\tau \to 0$.

In Mathematics (see, e.g., [10]) such solutions with singularities are usually studied in a space of functions with a finite norm involving a functional multiplier-the weight $\rho(\tau)$. The norm of the function $\rho(\tau)g(\tau)$ is then called the weighed norm of $g(\tau)$. The introduction of a weight $\rho(\tau)$ makes it possible to introduce into consideration the functions with infinite ordinary non-weighted norm. In most cases the

weight $\rho(\tau)$ tends to zero as its argument approaches the point of singularity $\tau = 0$; so, the simplest choice of the weights is $\rho(\tau) = \tau^{\nu}, \nu > 0$.

Note that in the literature on electrochemical impedance spectroscopy (EIS) the weighted solutions $\tau^{\nu} g(\tau), \nu = 1$ of the impedance equation (2) are of interest by themselves (see, e.g. [2, 6]) and often called as distribution functions of relaxation time (DFRT). Moreover, one is often interested in the behavior DFRT only within a time window $\tau \subseteq [W_{min}, W_{max}] \subset [0, \infty)$. Therefore, if $\tilde{g}(\tau)$is an approximate solution of the impedance equation (2), such as $\tilde{g}(\tau) = q_{\lambda_1,\lambda_2}(\tau)$, for example, then it seems to be reasonable to measure approximation error in the weighted norm

$$\|g - \tilde{g}\|_{L_{2,\nu}(W_{min},\ W_{max})} = \left\{ \int_{W_{min}}^{W_{max}} [\tau^{\nu}\, g(\tau) - \tau^{\nu} \tilde{g}(\tau)]^2 d\tau \right\}^{\frac{1}{2}}.$$

It is clear that this norm is a Hilbert space norm governed by the scalar product:

$$\langle f, g \rangle_{L_{2,\nu}(w_{min},W_{max})} = \int_{W_{min}}^{W_{max}} \tau^{2\nu} g(\tau) f(\tau) d\tau.$$

While we have described the explicit procedure (14), (15) for approximating the solutions of (2) directly from the impedance measurements, there is still a question about the choice of the regularization parameters λ_1, λ_2 that determine suitable relative weighting between these measurements. By setting $\lambda_1 = 0$ or $\lambda_2 = 0$, one may reduce this question to the case discussed in [4]. In another particular case $\lambda_1 = \lambda_2 = \lambda$, one may choose a suitable value of $\alpha = \lambda^{-1}$ by a cross-validation technique, as it was suggested in [6]. In both particular cases, one in fact deals with a single-parameter regularization, where many parameter choice strategies are available. A multi-parameter regularization is much less studied, especially when multiple regularization parameters are employed to construct a common misfit measure as in (5). In this direction one can only indicate the paper [8] and two references therein. Here we adjust the idea of [8] to the contexts of EIS.

Note that known regularization parameter choice strategies usually consist in using some criteria for selecting only one particular candidate from a family of approximate solutions calculated for different values of regularization parameters from sufficiently wide range. In contrast, in [8] it is proposed to construct a new approximate solution in the form of a linear combination of all calculated approximates. In the present context this means, for example, that at first we calculate $q_{\lambda_1,\lambda_2}(\tau)$ for some values $\lambda_1 = \lambda_{1,p},\ p = 0,1,2,\dots,P-1,\ \lambda_2 = \lambda_{2,q}, q = 0,1,2,\dots,Q-1,$, deserving consideration, and then consider a new approximate solution

$$\tilde{g}(\tau) = \sum_{m=0}^{PQ-1} c_m g^m(\tau), \tag{16}$$

where $g^m(\tau) = g_{\lambda_1,p,\lambda_2,q}(\tau),\ m = Pq + p,\ p = 0,1,2,\dots,P-1,\ q = 0,1,2,\dots,Q-1, m = 0,1,2,\dots,PQ-1$, and c_m are coefficients to be determined.

In view of the discussion above, it is natural to choose the coefficients c_m such that $\tilde{g}$ provides the best approximation of the exact solution g in the norm $\|\cdot\|_{L_{2,\nu}(W_{min}W_{max})}$ among all linear combinations (16). Since $\|\cdot\|_{L_{2,\nu}(W_{min}W_{max})}$ is a Hilbert space norm, it is clear that the coefficient vector $\vec{c} = (c_0, c_1, \dots, c_{PQ-1})$ should solve the following matrix vector equation:

$$G\vec{c} = \vec{F}, \tag{17}$$

where

$$\vec{F} = (F_m)_{m=0}^{PQ-1}, \qquad F_m = \langle g, g^m \rangle_{L_{2,\nu}(W_{min},W_{max})} = \int_{W_{min}}^{W_{max}} \tau^{2\nu} g(\tau) g^m(\tau) d\tau,$$

$$G = \left(G_{m,n}\right)_{m,n=0}^{PQ-1}, \qquad G_{m,n} = \langle g^m, g^n \rangle_{L_{2,\nu}(W_{min}, W_{max})} = \int_{W_{min}}^{W_{max}} \tau^{2\nu} g^m(\tau) g^n(\tau) d\tau.$$

If the regularized approximants

$$g^m(\tau) = g_{\lambda_1,p,\lambda_2,q}(\tau) = \sum_{j=0}^{2N-1} g_j^m l_j(\tau), \tag{18}$$

are already calculated from (14), (15), then the elements of the matrix G can be exactly calculated as well. Indeed, from (18) it follows that

$$G_{m,n} = \sum_{i=0}^{2N-1} \sum_{i=0}^{2N-1} g_i^m\, g_j^n b_{i,j},$$

where

$$b_{ij} = \langle l_i, l_j \rangle_{L_{2,\nu}(W_{min},W_{max})} = \int_{w}^{W} \tau^{2\nu} l_i(\tau) l_j(\tau) d\tau$$

and $l_i(\tau), l_j(\tau)$ are given by (11), (13). It is clear that the above integrals can be explicitly calculated. For example, for $\nu = 1$ and $i, j = N+1, \dots, 2N-1$ we have

$$b_{ij}=\begin{cases}\dfrac{W_{max}-W_{min}}{\omega_{i-N}\omega_{j-N}}+\dfrac{\omega_{j-N}^3\tan^{-1}(\omega_{i-N}\tau)-\omega_{i-N}^3\tan^{-1}(\omega_{j-N}\tau)}{\omega_{i-N}^2\omega_{j-N}^2(\omega_{i-N}^2-\omega_{j-N}^2)}\Big|_{\tau=W_{min}}^{\tau=W_{max}}, & i\neq j\\ \dfrac{\omega_{i-N}\tau\left(2+\left(1+\omega_{i-N}^2\tau^2\right)^{-1}\right)-3\tan^{-1}(\omega_{i-N}\tau)}{2\omega_{i-N}^3}\Big|_{\tau=W_{min}}^{\tau=W_{max}}, & i=j.\end{cases}$$

On the other hand, the components F_m of the vector $\vec{F}$ in (17) depend on the unknown solution g of (12), and therefore are inaccessible.

At the same time, in [8] and [11] we can find an approach to estimate the components of the vector $\vec{F}$ by using the so-called quasi-optimality criterion in the linear functional strategy. The advantage of this approach is that the values of the scalar products $F_m=\langle g,g^m\rangle_{L_{2,\nu}(W_{min},W_{max})}$ of the solution g can be estimated much more accurately than the solution g in the norm $\|\cdot\|_{L_{2,\nu}(W_{min}W_{max})}$.

According to [8, 11] we estimate the scalar product $\langle g,g^m\rangle$ by $\langle f_\alpha,g^m\rangle_{L_{2,\nu}(W_{min},W_{max})}$, where $f_\alpha(\tau)$ is the regularized approximate solutions $g_{\lambda_1,\lambda_2}(\tau)$ given by (14) and constructed for $\lambda_1=0,\lambda_2=\alpha$, with the use of only imaginary part of the impedance data. The reasons for this is that , as known in the literature (see, e.g. [2]) this part of data may allow better accuracy than the real part of the impedance.

In principle, the values of $\lambda_2=\alpha$ may be taken from the same set $\{\lambda_{2,q}\}_{q=0}^{Q-1}$ as the one above. But in [8, 11] it is suggested to take $\alpha=\alpha_s$ from a geometric sequence $\alpha_s=\alpha_0\beta^s, s=0,1,\dots,S-1, S>Q$. Therefore, we consider

$$f_s(\tau)=\sum_{j-N}^{2N-1}g_j^{0,s}\,l_j(\tau),$$

where $g_j=g_j^{0,s}$ are the solutions of the linear system (15) with $\lambda_1=0,\lambda_2=\alpha_s, s=0,1,\dots,S-1$, and

$$\langle f_s,g^m\rangle_{L_{2,\tau}(W_{min},W_{max})}=\sum_{i=N}^{2N-1}\sum_{j=0}^{2N-1}g_i^{0,s}\,g_j^m b_{i,j}.$$

Then, according to the quasi-optimality criterion in the linear functional strategy [11] we select such $s=s_m$ that

$$\left|\langle f_{s_m},g^m\rangle_{L_{2,\nu}(W_{min},W_{max})}-\langle f_{s_m-1},g^m\rangle_{L_{2,\nu}(W_{min},W_{max})}\right|$$
$$=min\left\{\left|\langle f_s,g^m\rangle_{L_{2,\nu}(W_{min},W_{max})}-\langle f_{s-1},g^m\rangle_{L_{2,\nu}(W_{min},W_{max})}\right|, s=1,2,\dots,S-1\right\}$$

The theoretical analysis of [11] quarantines that the values of $F_m=\langle g,g^m\rangle$ is well approximated by the values of $\widetilde{F_a}=\langle f_{s_m},g^m\rangle$. Recall that vector $\vec{c}$ of coefficients of the best linear combination of (16)

approximating the solution g of (2) in the norm $\|\cdot\|_{L_{2,\nu}(W_{min}W_{max})}$ should solve the matrix vector equation (17).

According to aggregation strategy [8] we approximate this ideal vector by the vector $\tilde{c} = (\tilde{c}_0, \tilde{c}_{1,\dots,}\tilde{c}_{PQ-1})$ solving in the least squares sense the approximate matrix vector equation

$$\mathrm{G}\tilde{c} = \widetilde{F}, \qquad \widetilde{F} = \left(\widetilde{F}_0, \widetilde{F}_1, \dots, \widetilde{F}_{PQ-1}\right). \tag{19}$$

Then the theoretical analysis of [8] quarantines that the approximate solution

$$\tilde{g}(\tau) = \sum_{m=0}^{PQ-1} \tilde{c}_m g^m(\tau) = \sum_{m=0}^{PQ-1}\sum_{j=0}^{N-1} \tilde{c}_m g_j^m \frac{1}{1+\omega_j^2\tau^2} + \sum_{m=0}^{PQ-1}\sum_{j=N}^{2N-1} \tilde{c}_m g_j^m \frac{\omega_{j-N}\tau}{1+\omega_{j-N}^2\tau^2}, \tag{20}$$

is almost as good as the best linear approximation (16) of the calculated regularized solutions $g_{\lambda_1,p,\lambda_2,q}(\tau)$.

Thus, we have described an adaptive procedure that automatically constructs an approximate solution of (2) and theoretically should perform at the level of the best regularized approximant $g_{\lambda_1,\lambda_2}(\tau)$ calculated according to (14), (15) for a given range of λ_1, λ_2. The input of the proposed procedure consists of the impedance data $Z(\omega_j), j = 0,1,\dots,N-1$, the weights γ_j, $j = 0,1,\dots,N-1$ determining the misfits measures, the endpoints W_{min}, W_{max} of the time window of interest, and the numbers $\lambda_{0,1}, \lambda_{0,2}, \alpha_0, P, Q, S$ defining the range of the regularization parameters under consideration.

3. Results

In this section we test the performances of the approximations (14), (15) and (20). For this purpose, we follow [5, 6] and employ analytically given impedance data $Z_{ex}(\omega)$ with known time relaxation characteristics $g(\tau)$ that solve (2). These synthetic experiments are based on single and double ZARC and Fractal element models [1]. To mimic the conditions of real EIS experiments, we add artificial noise to an analytical impedance $Z_{ex}(\omega)$ and use one of the models form [4, 12] such that noisy data are simulated as

$$Z(\omega_j) = Z_{ex}(\omega_j) + \varepsilon_j' + i\varepsilon_j'', \qquad j = 0,1,\dots,N-1. \tag{21}$$

where $\varepsilon_j', \varepsilon_j''$ are independent normally distributed random variables with zero mean and variance 10^{-4}; the frequencies are sampled from the range $\omega \subseteq [10^{-2}\mathrm{Hz}, 10^{6}\mathrm{Hz}]$ with 5 collocation points (ω_j) per decade.

3.1 Software tools used in this work

The new Distribution of Relaxation Time (DFRT) strategy was developed by open source Python 2.7.15 programming language [13] which is widely used in the science community [14-17]. The following essential Python open source modules were used in this work:

- Numpy [18] v1.14.3,
- Matplotlib [19] v2.2.2,
- wxPython v3.0.2.0,
- Cython 0.23.3 and
- PyInstaller v3.3.1.

The new DFRT approach was entirely coded from scratch and it relies heavily on NumPy module. However, other presented modules were necessary for data presentation and to embed the new DFRT strategy into the existing EisPy software package [20, 21].

3.2 Regularization (14), (15) with best tuned parameters

At first, we consider the situation, when in (14), (15) the regularization parameters λ_1, λ_2 are best-tuned for one of the models, say single ZARC element, and then used for other ones too. We discuss such an approach, because at first glance it may look as a reasonable parameter choice strategy, and at some extent it works, but not always. As in [6], we consider the impedance response of a single ZARC element model given by

$$Z_{ex}(\omega) = Z_{ex,\phi}(\omega, \tau_0) = \frac{R_{ct}}{1 + (i\omega\tau_0)^{\phi}}, \tag{22}$$

where $R_{ct} = 50\ \Omega, \tau_0 = 0.01\ s$ and $\phi = 0.7$. The corresponding solution $g(\tau)$ of (2) with $Z(\omega) = Z_{ex}(\omega)$ is given by

$$g(\tau) = \frac{R_{ct}}{2\pi\tau} \frac{\sin((1-\phi)\pi)}{\cosh\left(\phi log\left(\frac{\tau}{\tau_0}\right)\right) - \cos((1-\phi)\pi)}. \tag{23}$$

It turns out that the best reconstruction $g_{\lambda_1,\lambda_2}(\tau)$ of this solution from data (21) is given by (14), (15) with $\lambda_1 = 10^{-6}$, $\lambda_2 = 10^{8}$.

In Fig. 1 we plot DFRT $\gamma(\tau) = \tau g(\tau)$ and the corresponding point values of its approximation $\gamma_{\lambda_1,\lambda_2}(\tau) = \tau g_{\lambda_1,\lambda_2}(\tau)$ with best-turned parameters λ_1, λ_2.

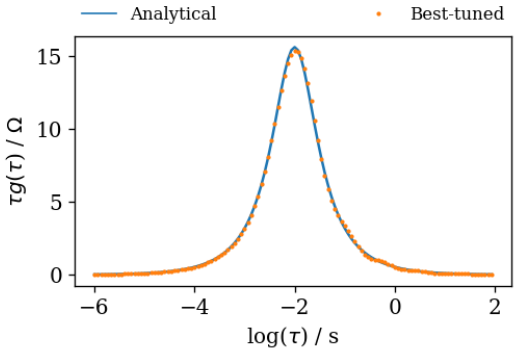

Fig. 1. Exact (—) DFRT of single ZARC element model and the corresponding approximation (·) with best-tuned parameters λ_1, λ_2.

Note that the above results and the ones reported below are obtained when in (15) the data misfits weights γ_k are chosen as

$$\gamma_k = |Z(\omega_k)|^{-2}, k = 0,1, \dots, N-1.$$

Such a choice has been advocated, for example, in [20].

In the next synthetic experiment we simulate noisy data (21) from single Fractal element model, where

$$Z_{ex}(\omega) = Z_{ex,\phi}(\omega, \tau_0) = \frac{R_{ct}}{(1 + i\omega\tau_0)^{\phi}}, \qquad (24)$$

and R_{ct}, τ_0 and ϕ are the same as in (22). Then the simulated data (21), (22) are used in the multi-parameter regularization (14), (15) with the same values λ_1, λ_2 that were best-tuned for the single ZARC element model (21), (22). The results are plotted in Fig. 2

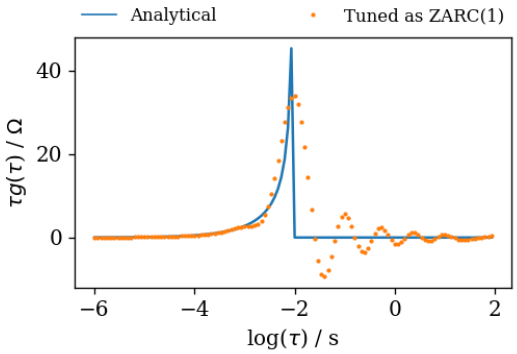

Figure 2. Exact (—) DFRT of single Fractal element model and the corresponding computed approximation (·) with parameters λ_1, λ_2, which are best-tuned for a single ZARC element model).

In Fig 2 the displayed oscillation in values of $\gamma_{\lambda_1,\lambda_2}(\tau) = \tau g_{\lambda_1,\lambda_2}(\tau)$ for $\tau > \tau_0 > 0.01(s)$ can be explained by the fact that in this experiment the corresponding exact solution

$$g(\tau) = \begin{cases} \frac{R_{ct}}{\pi} \frac{\sin(\phi\pi)}{\tau^{1-\phi}(\tau_0 - \tau)^{\phi}}, & if\ \tau < \tau_0 \\ 0, & if\ \tau > \tau_0, \end{cases} \qquad (25)$$

of the equation (2) has essential singularity not only at $\tau = 0$ but also at $\tau = \tau_0$. Therefore, such oscillations are common for other regularization techniques as well (see, e.g., [5]). On the other hand, Fig. 2 shows that for $\tau < \tau_0$ the approximation provided by λ_1, λ_2, that were best-tuned for single ZARC element model, is also quite good for the single Fractal element model.

At the same time, as we can see in the next example, it is not always reasonable to choose the regularization parameters λ_1, λ_2 *a priori*.

Consider synthetic data (21) simulated from a double ZARC element model, where

$$Z_{ex}(\omega) = Z_{ex,\phi}(\omega, \tau_{0,1}) + Z_{ex,\phi}(\omega, \tau_{0,2}), \qquad (26)$$

and the summands in (26) are given by (22) with $\tau_0 = \tau_{0,1} = 0.01\ (s), \tau_0 = \tau_{0,2} = 0.001\ (s)$. It is clear that the corresponding exact solution of (2) is just a sum of two functions (23) with $\tau_0 = \tau_{0,1}, \tau_{0,2}$. If we now take the previous values of λ_1, λ_2 and apply regularization (14), (15) to the data (21), (26), then we obtain the result displayed in Fig. 3, which does not allow a proper detection of the numbers of different time constants (peaks) and their values (location) $\tau_{0,1}, \tau_{0,2}$. This example, provides a motivation for employing the aggregation procedure described in Section 2.2.

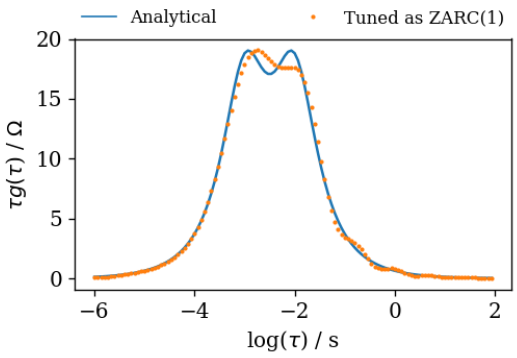

Fig. 3. Exact (—) DFRT of double ZARC element model and the corresponding computed approximation (·) with parameters λ_1, λ_2, which are best-tuned for a single ZARC element model.

3.3 Performance of the aggregated approximation (20)

The aggregation procedure resulting in the approximation (20), is illustrated with the following values of the input parameters:

$$\lambda_{1,p} = 10^{p-7}, p = 0,1,2;\ \lambda_{2,q} = 10^{5+q}, q = 0,1,2,\dots,5;$$

$$\alpha_s = \alpha_0\beta^s, s = 0,1,2,\dots,9;\ \alpha_0 = 3.2\cdot 10^4, \beta = 0.2\,;$$

$$W_{min} = 10^{-2}, W_{max} = 10^2.$$

This means that altogether, 28 regularized approximate solutions (14), (15) need to be computed for each collocation dataset $\{Z(\omega_j)\}$, among them 18 approximants g_{λ_1,λ_2} with $\lambda_1 = \lambda_{1,p}, \lambda_2 = \lambda_{2,q}$ are aggregated in (20), and the remaining 10 approximants g_{λ_1,λ_2} with $\lambda_1 = 0,\ \lambda_2 = \alpha_s$ are used as $f_s = g_{0,\alpha_s}$ for defining a vector $\tilde{F}$ in (19).

The illustration of the aggregation procedure is produced for two collocation datasets. One of them has been simulated from a double ZARC element model and discussed in the previous subsection as a motivation for the use of the aggregation procedure. The second one is simulated from a double Fractal element model in the same way as (21), (26). The only difference is that this time the summands in (26) are given by (*24*) with $\tau_0 = \tau_{0,1}, \tau_{0,2}$. The inputs described above are used in the aggregation procedure from Section 2.2. The aggregation is performed in the weighted norms $\|\cdot\|_{L_{2,\nu}(W_{min}W_{max})}$ with the weights $\rho(\tau) = \tau^\nu, \nu = 0,1,2$. This means that three systems (19) need to be formed and solved (one for each ν) to find the coeficients g_j^n in (*20*). Note that no additional regularized approximants are computed for this. The results are displayed in Fig. 4 (double ZARC element model) and in Fig. 5 (double Fractal element model).

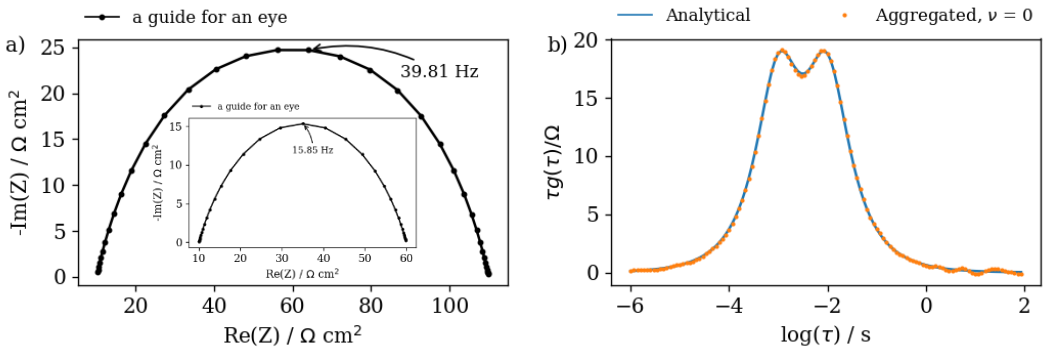

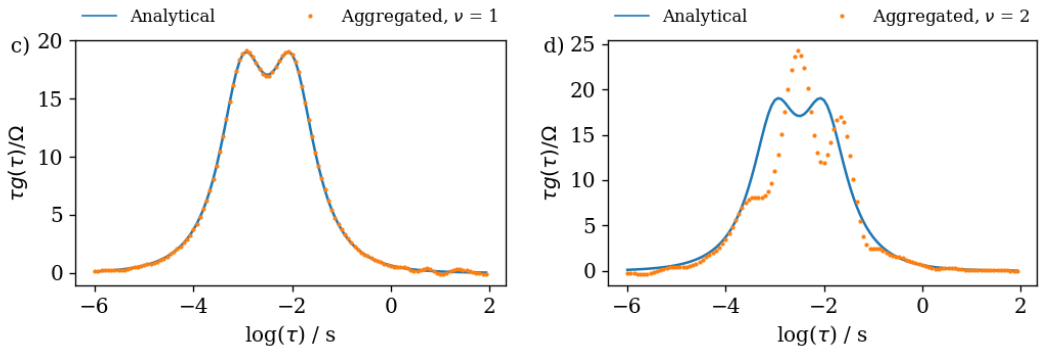

Fig. 4. The synthetic impedance data of double ZARC element model (a) and corresponding exact (—) and the approximated DFTR, produced by the aggregation in different norms (b-d). The synthetic data of single ZARC element is presented in inset of subplot (a).

These results show that the aggregation performed in one of the considered norms ($\|\cdot\|_{L_{2,2}}$ in the case of ZARC, and $\|\cdot\|_{L_{2,0}}$ in the case of Fractal) does not produce good approximation and differs essentially from the other ones.

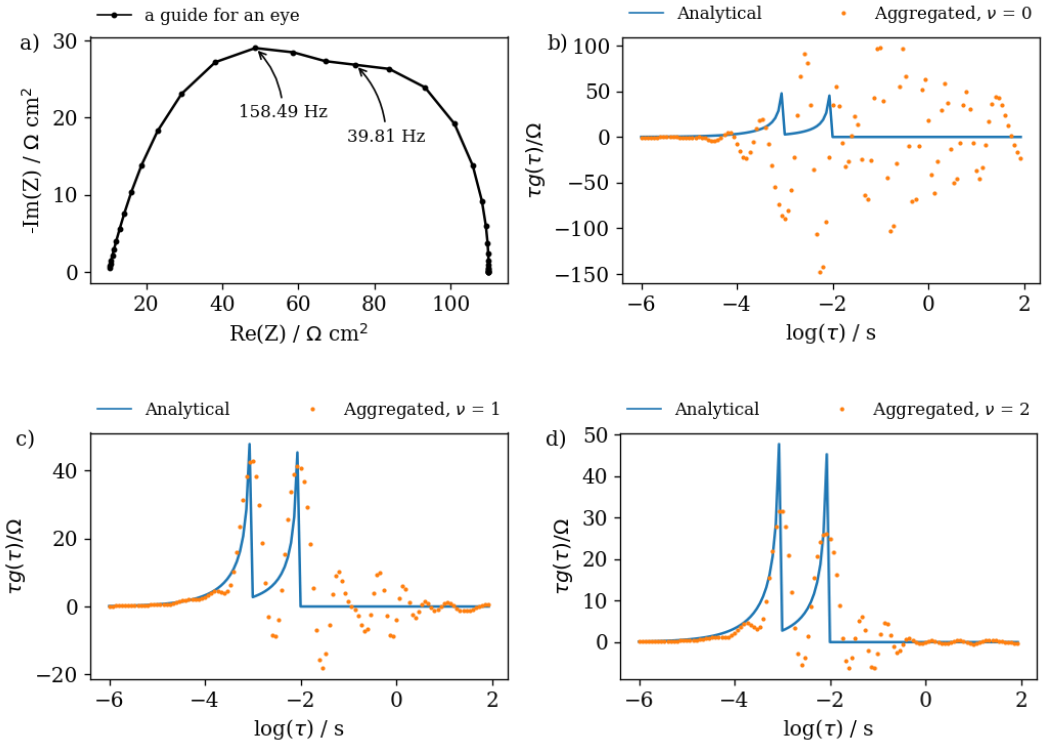

Fig. 5. The synthetic impedance data of double Fractal element model (a) and corresponding exact (—) and the approximated DFTR, produced by the aggregation in different norms (b-d).

At the same time, for two other norms the aggregation results are very similar and quite accurate. This observation hints at the possibility that the approximations produced by the aggregation in different norms can be seen as a kind of "expert opinions". Then the decision upon the output of the whole aggregation procedure can be made by "majority voting".

In Fig. 5 one can see the result of the regularization (14), (15) corresponds to the values $\lambda_1 = 10^{-6}, \lambda_2 = 10^{10}$ that are the best tuned to the reconstruction from the considered data, which have been simulated from double Fractal element model. This result is quite similar to the one obtained in the aggregation after the above mentioned "majority voting" and supports the theoretical claim that the aggregated approximant (20) is almost as good as the best approximant involved in the aggregation procedure.

At the end, we would like to highlight one more feature of the aggregated approximation (20), namely its ability to properly determine the number of time constants involved in the models under consideration (i.e. the peaks in DFTR shapes) from similar looking impedance spectra.

To illustrate this, we observe that the impedance spectra of single and double ZARC element models (inset in Fig. 4a and Fig. 4a) look very similar, such that their visual inspection does not reveal a difference in numbers of peaks of corresponding DFRT shapes. At the same time, the aggregation procedure resulting in the approximation (20) automatically detects the above mentioned difference (see right panels of Fig. 1 and Fig. 4bc) without any changes in input parameters $\lambda_{1,p}, \lambda_{2,g}, \alpha_s, W_{min}, W_{max}$.

4. Conclusion

In this article, we have proposed a novel scheme for estimating DFRT based on multi-penalty regularization. The performance of the proposed scheme depends on the choice of involved regularization parameters.

The usual approach to such a choice is to compute approximate solutions for several parameter values and then select only one of them according to some criterion. In this article we have followed another strategy and employed a recent idea [8, 11] that uses all computed approximate solutions to construct a new one performing at the level of the best, but unknown, computed approximation.

The application of this idea is not restricted to the proposed scheme. A possible scenario may be the combination of different approximations, such as [3-5], by using the same aggregation strategy.

Another novelty of the article is the observation that no additional discretization is necessary when dealing with collocated equations of DFRT problem. This observation allows direct implementation of

the proposed multi-penalty regularization scheme such that all appearing quantities, except design parameters, can be calculated exactly/symbolically. Based on our discussion of the synthetic experiments, we conclude that the proposed scheme exhibits expected performance and can be implemented in the form of a toolbox.

With intention to enable wider usage of the toolbox, it has been embedded in the free EisPy v.3.01 software package which is openly shared online [22] under the MIT license[1].

Acknowledgments

M.Ž gratefully acknowledges the stimulation program "Joint Excellence in Science and Humanities" (JESH) of the Austrian Academy of Sciences for providing supporting funds. S.P.Jr. acknowledges the support of Austrian Science Fund (FWF), Project P 29514. Both authors express their gratitude to Prof. Dr. Sergei Pereverzyev (the JESH-host scientist at RICAM) for fruitful suggestions and valuable comments.

5. References

[1] E. Barsoukov, J.R. Macdonald, Impedance Spectroscopy: Theory, Experiment, and Applications, 2005.

[2] F. Dion, A. Lasia, The use of regularization methods in the deconvolution of underlying distributions in electrochemical processes, Journal of Electroanalytical Chemistry 475(1) (1999) 28-37.

[3] R.A. Renaut, R. Baker, M. Horst, C. Johnson, D. Nasir, Stability and error analysis of the polarization estimation inverse problem for microbial fuel cells, Inverse Problems 29(4) (2013).

[4] A.L. Gavrilyuk, D.A. Osinkin, D.I. Bronin, The Use of Tikhonov Regularization Method for Calculating the Distribution Function of Relaxation Times in Impedance Spectroscopy, Russian Journal of Electrochemistry 53(6) (2017) 575-588.

[5] M. Saccoccio, T.H. Wan, C. Chen, F. Ciucci, Optimal Regularization in Distribution of Relaxation Times applied to Electrochemical Impedance Spectroscopy: Ridge and Lasso Regression Methods - A Theoretical and Experimental Study, Electrochimica Acta 147 (2014) 470-482.

[1] See: https://opensource.org/licenses/MIT.

[6] T.H. Wan, M. Saccoccio, C. Chen, F. Ciucci, Influence of the Discretization Methods on the Distribution of Relaxation Times Deconvolution: Implementing Radial Basis Functions with DRTtools, Electrochimica Acta 184 (2015) 483-499.

[7] P. Mathe, S.V. Pereverzev, Discretization strategy for linear ill-posed problems in variable Hilbert scales, Inverse Problems 19(6) (2003) 1263-1277.

[8] J.Y. Chen, S. Pereverzyev, Y.S. Xu, Aggregation of regularized solutions from multiple observation models, Inverse Problems 31(7) (2015).

[9] K.S. Cole, R.H. Cole, Dispersion and absorption in dielectrics I. Alternating current characteristics, Journal of Chemical Physics 9(4) (1941) 341-351.

[10] L.D.K. (originator), Encyclopedia of Mathematics : Weighted space, 1993. http://www.encyclopediaofmath.org/index.php?title=Weighted_space&oldid=15433.

[11] S. Kindermann, S. Pereverzyev, Jr., A. Pilipenko, The quasi-optimality criterion in the linear functional strategy, ArXiv e-prints, 2017.

[12] F. Ciucci, C. Chen, Analysis of Electrochemical Impedance Spectroscopy Data Using the Distribution of Relaxation Times: A Bayesian and Hierarchical Bayesian Approach, Electrochimica Acta 167 (2015) 439-454.

[13] T.E. Oliphant, Python for scientific computing, Computing in Science & Engineering 9(3) (2007) 10-20.

[14] D.S. Cao, Q.S. Xu, Q.N. Hu, Y.Z. Liang, ChemoPy: Freely available python package for computational biology and chemoinformatics, Bioinformatics 29(8) (2013) 1092-1094.

[15] J.J. Helmus, C.P. Jaroniec, Nmrglue: An open source Python package for the analysis of multidimensional NMR data, Journal of Biomolecular NMR 55(4) (2013) 355-367.

[16] D.S. Cao, Q.S. Xu, Y.Z. Liang, Propy: A tool to generate various modes of Chou's PseAAC, Bioinformatics 29(7) (2013) 960-962.

[17] J. Kieffer, J.P. Wright, PyFAI: A python library for high performance azimuthal integration on GPU, Powder Diffraction 28(SUPPL.2) (2013) S339-S350.

[18] S. van der Walt, S.C. Colbert, G. Varoquaux, The NumPy Array: A Structure for Efficient Numerical Computation, Computing in Science & Engineering 13(2) (2011) 22-30.

[19] J.D. Hunter, Matplotlib: A 2D graphics environment, Computing in Science & Engineering 9(3) (2007) 90-95.

[20] M. Zic, An alternative approach to solve complex nonlinear least-squares problems, Journal of Electroanalytical Chemistry 760 (2016) 85-96.
[21] M. Zic, Solving CNLS problems by using Levenberg-Marquardt algorithm: A new approach to avoid off-limits values during a fit, Journal of Electroanalytical Chemistry 799 (2017) 242-248.
[22] EisPy v.3.01 is hosted on https://goo.gl/j5nizb.